

Topological Crystalline Insulators

Liang Fu

Department of Physics, Harvard University, Cambridge, MA 02138

The recent discovery of topological insulators has revived interest in the topological properties of insulating band structures. In this work, we extend the topological classification of insulating band structures to include certain point group symmetry of crystals. We find a class of three-dimensional “topological crystalline insulators” which have metallic surface states on certain high symmetry crystal surfaces. These topological crystalline insulators can be viewed as the counterpart of topological insulators in materials without spin-orbit coupling. Their surface states have quadratic band degeneracy instead of linear Dirac dispersion. Their band structures are characterized by new Z_2 invariants. We hope this work will enlarge the family of topological phases in band insulators and stimulate the search for them in real materials.

PACS numbers: 73.20.-r, 73.43.-f

The topological property of insulating band structures has played an important role in the study of topological phases of matter. Historically the quantization of Hall conductance in the integer quantum Hall effect was explained by the TKNN topological invariant[1]. Recently the topological classification of spin-orbital coupled band structures with time reversal symmetry has led to the theoretical prediction of topological insulators[2–5]. The subsequent development of topological band theory[6], combined with realistic band structure calculations, has proven useful in the material search for topological insulators[7–9].

Inspired by the discovery of topological insulators, fermion band structures in different symmetry classes and spatial dimensions have been mathematically classified, and topologically nontrivial phases have been found. Notable examples include topological superconductors[10, 11] and topological antiferromagnetic insulators[12]. Finding these phases in real materials is interesting and challenging.

The purpose of this work is to extend the classification of band structures in a different direction—to include the point group symmetry of crystals. We introduce the notion of “topological crystalline insulators”, which cannot be smoothly connected to a trivial atomic insulator when time reversal (T) symmetry and certain point group symmetry are respected. Because sample edges or surfaces often break crystal symmetries, topological crystalline insulators defined in the above sense do not have protected surface states in general. Nonetheless, we find a class of topological crystalline insulators in three dimensions with a four-fold (C_4) or six-fold (C_6) rotation axis (c -axis), which have hallmark surface states on the (001) crystal face. These topological crystalline insulators are the counterpart of topological insulators in materials *without spin-orbit coupling*, but with electron’s orbitals playing a role similar to spin. The (001) surface states of topological crystalline insulators have *quadratic* band degeneracy protected by time reversal and discrete rotational symmetry[13, 14].

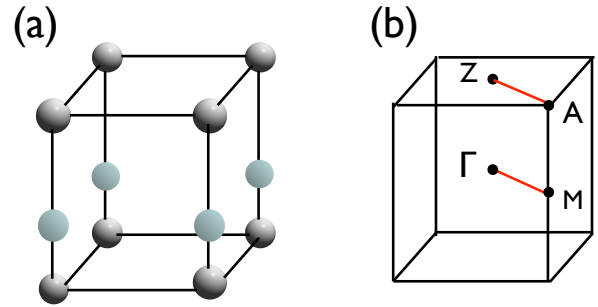


FIG. 1: (a) tetragonal lattice with two atoms A and B along the c -axis in the unit cell; (b) the Brillouin zone and four high symmetry points.

The outline of this paper is as follows. First we introduce a simple tight-binding model in a tetragonal crystal with C_4 symmetry. We explicitly show that gapless surface states exist on the (001) crystal face. The topological stability of surface states suggests a nontrivial phase in this model. Next we define a new Z_2 topological invariant for T - and C_4 -invariant band structures in three dimensions. This establishes the topological crystalline insulator phase. We also discuss generalizations of the tight-binding model and the Z_2 invariant to crystals with C_6 symmetry. Finally, we compare the quadratic surface band of topological crystalline insulators with bilayer graphene and discuss its electronic properties.

Tight-Binding Model: Consider a tetragonal lattice with a unit cell of two inequivalent atoms A and B along c -axis, as shown in Fig.1a. The 3D crystal can be viewed as a stack of bilayer square lattices in the ab plane. We now introduce a tight-binding model to describe the band structure of electron’s p orbitals (or d orbitals, see the next paragraph). In particular, we are interested in the energy bands derived from p_x and p_y orbitals. Assuming that these bands do not overlap with the p_z bands, we construct the tight-binding Hamiltonian H from p_x and p_y orbitals[15]. H consists of intra-layer hopping H^A and

H^B , as well as inter-layer hopping H^{AB} :

$$\begin{aligned}
H &= \sum_n H_n^A + H_n^B + H_n^{AB}, \\
H_n^a &= \sum_{i,j} t^a(\mathbf{r}_i - \mathbf{r}_j) \sum_{\alpha,\beta} c_{a\alpha}^\dagger(\mathbf{r}_i, n) e^{ij} e_{\beta}^{ij} c_{a\beta}(\mathbf{r}_j, n), \\
H_n^{AB} &= \sum_{i,j} t'(\mathbf{r}_i - \mathbf{r}_j) \left[\sum_{\alpha} c_{A\alpha}^\dagger(\mathbf{r}_i, n) c_{B\alpha}(\mathbf{r}_j, n) + h.c. \right] \\
&\quad + t'_z \sum_i \sum_{\alpha} [c_{A\alpha}^\dagger(\mathbf{r}_i, n) c_{B\alpha}(\mathbf{r}_i, n+1) + h.c.] \quad (1)
\end{aligned}$$

Here each site is specified by (n, \mathbf{r}, a) : n labels the bilayer unit cell along c -axis; $\mathbf{r} = (x, y)$ labels the ab -plane coordinate; $a = A, B$ labels the sublattice. $\alpha = p_x, p_y$ labels the orbital. Two types of p -orbital hopping terms appear in H . The intra-layer hopping in H^a is of σ -bonding type: it depends on the relative orientation of p -orbital and the hopping direction $\mathbf{e}^{ij} = (\mathbf{r}_i - \mathbf{r}_j)/|\mathbf{r}_i - \mathbf{r}_j|$. The inter-layer hopping in H^{AB} is orbital-independent. Written in this form, the hopping terms manifestly preserve crystal symmetries. The hopping amplitudes t^a , t' and t'_z between two sites depend on their ab -plane distance $\mathbf{r}_i - \mathbf{r}_j$. Throughout this work, we assume spin-orbit coupling is negligible, so that electron's spin index is omitted.

We note that the form of the Hamiltonian (1) is determined by the transformation properties of $p_{x,y}$ orbitals under C_4 symmetry. Therefore (1) also applies to electrons in $d_{xz,yz}$ orbitals. This opens up the exciting possibility of realizing the model Hamiltonian in transition metal compounds with active e_g orbitals.

To obtain a minimal model for topological crystalline insulators, we include the nearest and next-nearest neighbor intra-layer hoppings in H^a with the amplitude t_1^a and t_2^a , as well as nearest and next-nearest neighbor inter-layer hoppings in H^{AB} with the amplitude t'_1 and t'_2 , as shown in Fig.1b. The corresponding Bloch Hamiltonian $H(\mathbf{k})$ is obtained by Fourier transform:

$$\begin{aligned}
H(\mathbf{k}) &= \begin{pmatrix} H^A(\mathbf{k}) & H^{AB}(\mathbf{k}) \\ H^{AB\dagger}(\mathbf{k}) & H^B(\mathbf{k}) \end{pmatrix} \\
H^a(\mathbf{k}) &= 2t_1^a \begin{pmatrix} \cos k_x & 0 \\ 0 & \cos k_y \end{pmatrix} \\
&\quad + 2t_2^a \begin{pmatrix} \cos k_x \cos k_y & \sin k_x \sin k_y \\ \sin k_x \sin k_y & \cos k_x \cos k_y \end{pmatrix}, \\
H^{AB}(\mathbf{k}) &= [t'_1 + 2t'_2(\cos k_x + \cos k_y) + t'_z e^{ik_z}] I, \quad (2)
\end{aligned}$$

where we have introduced $\sigma_z = \pm 1$ to denote the $p_x(p_y)$ orbitals, and $\tau_z = \pm 1$ to denote the A(B) sublattice. The band structure is shown in Fig.2a for the following set of parameters: $t_1^A = -t_1^B = 1, t_2^A = -t_2^B = 0.5, t'_1 = 2.5, t'_2 = 0.5, t'_z = 2$. We have checked that the energy gap is finite everywhere in the Brillouin zone. As long as the energy gap does not close, the system remains in the same topological class within a finite parameter range.

To study surface states, we solve H in a slab geometry. We find that the existence of gapless surface states

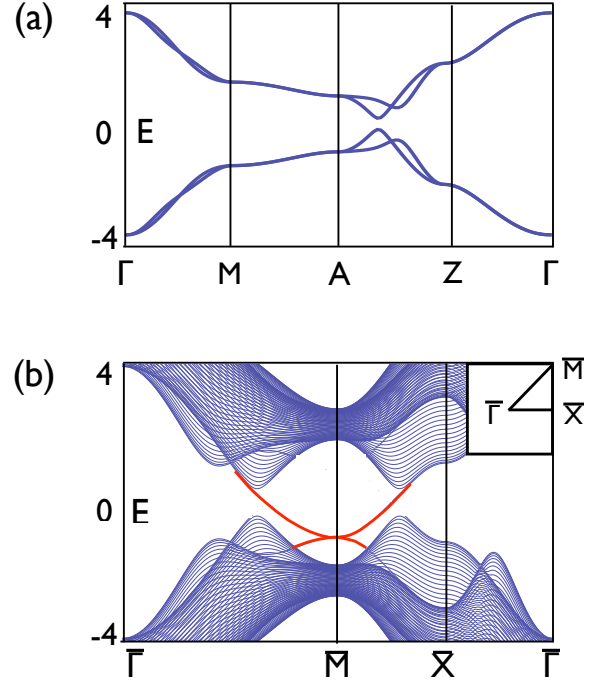


FIG. 2: (a) bulk band structure of the tight binding model along high symmetry lines; (b) surface states with quadratic band touching exist on (001) face. The tight-binding parameters are $t_1^A = -t_1^B = 1, t_2^A = -t_2^B = 0.5, t'_1 = 2.5, t'_2 = 0.5, t'_z = 2$.

crucially depend on the surface termination. Consider the high symmetry (001) surface, which preserves the C_4 symmetry. Here surface states exist and transverse the whole energy gap as shown in Fig.2, leading to a 2D surface metal. Note that surface states are doubly degenerate at $\bar{M} = (\pi, \pi)$: one in p_x orbital and the other in p_y orbital. Because \bar{M} is a fixed point under four-fold rotation, the doublet form a two-dimensional irreducible *real* representation of C_4 symmetry, as a result of time reversal symmetry for electrons without spin-orbit coupling (i.e., spinless fermions). Surface band dispersion near \bar{M} is quadratic. This can be understood from $k \cdot p$ theory. By choosing an appropriate basis at \bar{M} , the $k \cdot p$ Hamiltonian can be brought to the standard form

$$H_{\text{eff}}(k_x, k_y) = \frac{k^2}{2m^*} + \alpha(k_x^2 - k_y^2)\gamma_z + \beta k_x k_y \gamma_x. \quad (3)$$

In this basis, C_4 is represented by $e^{i\sigma_y\pi/4}$ and time reversal operator T is represented by complex conjugation. Perturbations that break either C_4 or T symmetry can open up an energy gap and destroy the metallic surface states. This can be seen explicitly by adding a C_4 -breaking term $M_1 k_x \gamma_y + M_2 \gamma_z$ or a T -breaking term $M \gamma_y$ to H_{eff} . Therefore the gapless surface states on (001) surface are protected by C_4 and T symmetry. Similar symmetry-protected quadratic bands have been recently studied in 2D photonic crystals[13] and fermion

models[14]. For other surface terminations which break the C_4 symmetry, our tight-binding model does not have gapless surface states.

In the absence of symmetry-breaking perturbations, the surface states are protected for a topological reason. This can be understood by considering the surface band dispersion along $\bar{\Gamma}\bar{M}$. Within our model, surface states (if present) must be doubly degenerate at $\bar{\Gamma}$ and \bar{M} [16]. As a consequence, there exists two distinct types of surface band connectivity along $\bar{\Gamma}\bar{M}$, having an even or odd number of band crossings at Fermi energy respectively. The former type of surface states are fragile: they can be pushed out of the energy gap by changing the surface potential. The latter type of surface states have a Fermi surface that encloses $\bar{\Gamma}$ or \bar{M} an odd number of times. They cannot be removed, and hence the topological protection. These two types of surface states imply the existence of two topologically distinct phases of time-reversal-invariant band insulators with four-fold symmetry. The reasoning here closely follows the previous study of topological insulators[17].

Z_2 Topological Invariant: We now show that the two phases are distinguished by the topological property of electron wavefunctions in the ground state. We find that a new Z_2 topological invariant $\nu_0 = \pm 1$ characterizes the band structure of 3D time-reversal-invariant insulators with four-fold rotation symmetry (without spin-orbit coupling). In particular, $\nu_0 = -1$ corresponds to a topological crystalline insulator which has gapless surface states on the (001) surface.

We start by examining the symmetry property of Bloch wavefunctions of occupied bands: $|\psi_n(\mathbf{k})\rangle = e^{i\mathbf{k}\cdot\mathbf{r}}|u_n(\mathbf{k})\rangle$, where $|u_n(\mathbf{k})\rangle$ is the cell-periodic eigenstates of the Bloch Hamiltonian $H(\mathbf{k}) \equiv e^{-i\mathbf{k}\cdot\mathbf{r}}He^{i\mathbf{k}\cdot\mathbf{r}}$. Here the unit cell is chosen to be invariant under C_4 rotation around the axis $x = y = 0$. $H(\mathbf{k})$ satisfies

$$\begin{aligned} H(k_x, k_y, k_z) &= UH(k_y, -k_x, k_z)U^{-1} \\ H(k_x, k_y, k_z) &= TH(-k_x, -k_y, -k_z)T^{-1}. \end{aligned} \quad (4)$$

Here the unitary operator $U = e^{i(\hat{P}_x y - \hat{P}_y x)\pi/2}$ implements C_4 rotation within the unit cell. The anti-unitary operator $T = K$ (complex conjugation) implements time reversal transformation for *spinless* fermions, with the property $T^2 = 1$. As a result, time reversal symmetry by itself does not guarantee a two-fold degeneracy. However, the combination of time reversal and four-fold rotational symmetry can lead to protected degeneracies at four special momenta $\Gamma = (0, 0, 0)$, $M = (\pi, \pi, 0)$, $A = (\pi, \pi, \pi)$, $Z = (0, 0, \pi)$ in the 3D Brillouin zone (Fig.1b). At such a high symmetry point \mathbf{k}_i , $H(\mathbf{k}_i)$ is real and commutes with U , so that the energy bands $|u_n(\mathbf{k}_i)\rangle$ form irreducible *real* representations of C_4 group. The dimension of the representation determines the multiplicity of the degeneracy. C_4 group has two distinct one-dimensional representations and a two-dimensional

representation. The latter corresponds to a pair of doubly degenerate states which transform into each other under C_4 , e.g. (p_x, p_y) orbitals or (d_{xz}, d_{yz}) orbitals. From now on, we only consider occupied energy bands $|u_n(\mathbf{k})\rangle$, $n = 1, \dots, 2N$ which are doubly degenerate at Γ, M, A, Z so that each doublet belongs to the two-dimensional representation of C_4 group. As we will see below, only such band structures admit a Z_2 classification.

The Z_2 topological invariant ν is defined in terms of the electron wavefunctions:

$$\begin{aligned} \nu_0 &= \nu_{TM}\nu_{AZ}, \\ \nu_{\mathbf{k}_1\mathbf{k}_2} &= \exp(i \int_{\mathbf{k}_1}^{\mathbf{k}_2} d\mathbf{k} \cdot \mathcal{A}_{\mathbf{k}}) \frac{\text{Pf}[w(\mathbf{k}_2)]}{\text{Pf}[w(\mathbf{k}_1)]}, \\ \mathcal{A}_{\mathbf{k}} &\equiv -i \sum_j \langle u_j(\mathbf{k}) | \partial_{\mathbf{k}} | u_j(\mathbf{k}) \rangle, \\ w_{mn}(\mathbf{k}_i) &\equiv \langle u_m(\mathbf{k}_i) | UT | u_n(\mathbf{k}_i) \rangle. \end{aligned} \quad (5)$$

$\mathcal{A}_{\mathbf{k}}$ is the $U(1)$ Berry connection. $w(\mathbf{k}_i)$ is a $U(2N)$ matrix, as seen from the the symmetry properties of $H(\mathbf{k}_i)$. We now specify the integration path in (6). For ν_{TM} , the integral is along an arbitrary line connecting Γ and M which lies *within* the 2D plane $k_z = 0$ in the Brillouin zone as shown in Fig.1b. Likewise, the integration path for ν_{AZ} lies in the plane $k_z = \pi$.

Both \mathcal{A} and w depend on the choice of basis $|u_j(\mathbf{k})\rangle$, but we now prove that $\nu_{\mathbf{k}_1\mathbf{k}_2}$ is gauge invariant. Two different basis $|\tilde{u}_n(\mathbf{k})\rangle$ and $|u_n(\mathbf{k})\rangle$ are related by a $U(2N)$ gauge transformation:

$$|\tilde{u}_n(\mathbf{k})\rangle = \mathcal{G}_{nm}(\mathbf{k})|u_m(\mathbf{k})\rangle, \quad \mathcal{G} \in U(2N) \quad (7)$$

This leads to the corresponding gauge transformation of \mathcal{A} and w :

$$\begin{aligned} \tilde{\mathcal{A}} &= \mathcal{A} - i\text{Tr}[\mathcal{G}^{-1}\partial_{\mathbf{k}}\mathcal{G}] = \mathcal{A} - i\partial_{\mathbf{k}} \log(\det[\mathcal{G}]) \\ \tilde{w} &= \mathcal{G}^* w \mathcal{G}^\dagger \end{aligned} \quad (8)$$

Using the identity $\text{Pf}[X^T M X] = \det[X]\text{Pf}[M]$, it is straightforward to verify that $\tilde{\nu}_{\mathbf{k}_1\mathbf{k}_2} = \nu_{\mathbf{k}_1\mathbf{k}_2}$ is gauge invariant.

We now further show that $\nu_{\mathbf{k}_1\mathbf{k}_2} = \pm 1$ is a Z_2 quantity. It follows from (4) that at the two 2D planes $k_z = 0$ and $k_z = \pi$, $H(\mathbf{k})$ has the symmetry property: $H(\mathbf{k}) = \Xi H(\mathbf{k})\Xi$, $\Xi \equiv U^2 T$. This allows us to choose a *real* gauge along the integration path to evaluate (6):

$$\Xi|u_m(\mathbf{k})\rangle = -|u_m(\mathbf{k})\rangle, \quad (9)$$

Because Ξ is anti-unitary, $\mathcal{A} = 0$ everywhere along the integration path. So in this gauge $\nu[\mathbf{k}_1, \mathbf{k}_2]$ reduces to

$$\nu_{\mathbf{k}_1\mathbf{k}_2} = \text{Pf}[w(\mathbf{k}_2)]/\text{Pf}[w(\mathbf{k}_1)]. \quad (10)$$

Because $|u_m(\mathbf{k}_i)\rangle$ belong to the two-dimensional representation of C_4 group, we have $U^2|u_m(\mathbf{k}_i)\rangle = -|u_m(\mathbf{k}_i)\rangle$,

so that the gauge condition (9) at \mathbf{k}_i is equivalent to $T|u_m(\mathbf{k}_i)\rangle = |u_m(\mathbf{k}_i)\rangle$, i.e., the wavefunction is real. Under this reality condition, the matrix $w(\mathbf{k}_i)$ simplifies to

$$w_{mn}(\mathbf{k}_i) = \langle u_m(\mathbf{k}_i)|U|u_n(\mathbf{k}_i)\rangle. \quad (11)$$

Now by choosing a particular kind of real basis $|u_{2m}(\mathbf{k}_i)\rangle \equiv U|u_{2m-1}(\mathbf{k}_i)\rangle$, $w(\mathbf{k}_i)$ reduces to a standard form $w^0 = \epsilon \oplus \epsilon \dots \oplus \epsilon$, which is a direct sum of $N \times 2 \times 2$ Levi-Civita tensors. This means that in a generic real basis, $w(\mathbf{k}_i)$ can be written as

$$w(\mathbf{k}_i) = O^T(\mathbf{k}_i)w^0O(\mathbf{k}_i), \quad O(\mathbf{k}_i) \in O(2N). \quad (12)$$

So we have

$$\text{Pf}[w(\mathbf{k}_i)] = \det[O(\mathbf{k}_i)]\text{Pf}[w^0] = \det[O(\mathbf{k}_i)] = \pm 1. \quad (13)$$

This proves that $\nu_{\mathbf{k}_1\mathbf{k}_2} = \pm 1$ is a gauge invariant Z_2 quantity. So both $\nu_{\Gamma M}$ and ν_{AZ} are Z_2 topological invariants which characterize the band structures in the 2D momentum space $k_z = 0$ and $k_z = \pi$ respectively. While ν is essentially a topological invariant for 2D insulators, their product ν_0 is only defined for 3D time-reversal-invariant insulators with C_4 symmetry. Moreover, ν_0 determines the surface state property: gapless surface states exist on (001) face only when $\nu_0 = -1$. This is verified in the tight-binding model (1). The relation between ν_0 and ν is analogous to that of strong and weak Z_2 index in 3D topological invariants[3–5].

Generalization to Crystals with C_6 Symmetry:

The study of topological crystalline insulators with C_4 symmetry can be easily generalized to hexagonal crystal structures with C_6 symmetry. In that case, topologically protected (001) surface states have quadratic degeneracy points either at $\bar{\Gamma}$ or two equivalent \bar{K} . The corresponding topological invariant is also defined by Eq.(5,6) from the electron wavefunctions on the lines ΓK and AH in the Brillouin zone. A concrete example of topological crystalline insulators with C_6 symmetry can be obtained by placing the tight-binding model (1) in a layered triangular lattice. The details will be reported elsewhere.

Topological crystalline insulators are likely to exist in other crystal structures as well. We hope this work will stimulate future studies to map out a complete phase space for topological phases in crystalline insulators.

Surface States with Quadratic Degeneracy:

Quadratic degeneracies in 2D band structure have attracted considerable interest recently. The $k \cdot p$ Hamiltonian (3) is widely used as a low energy theory near $\pm K$ points for bilayer graphene. However, unlike the surface states of topological crystalline insulators, the quadratic degeneracy in bilayer graphene is *not* protected by symmetry. In fact, it is known that the band dispersion of bilayer graphene very close to $\pm K$ becomes linear instead of quadratic due to trigonal warping effects.

When electron interactions are included, the quadratic surface states can spontaneously generate a mass gap,

leading to a variety of possible interesting broken symmetry phases including quantum anomalous Hall state, nematic phase and etc[14]. The competition between different ordered phases is currently being studied in bilayer graphene. It will be interesting to see what happens in the *single-valley* quadratic surface states of topological crystalline insulators.

The fate of surface states in the presence of disorder is another open problem. Because the 2D surface states studied here belong to the orthogonal class, one may expect that all single-particle states are localized for arbitrarily small amount of disorder. However, we suspect that the localization/delocalization issue depends on the types of disorder. We leave this problem to future studies.

It is also interesting to generalize the concept of topological crystalline insulators to interacting systems. For example, crystal symmetry is known to play an important role in the topological classification of spin liquids[18], spin chains[19], and Mott insulators[20]. A unifying theory of symmetry protected topological order remains to be developed.

Part of this work was done in early 2009 at University of Pennsylvania under the support of NSF grant DMR-0906175. We thank Charlie Kane and Jeffrey Teo for very helpful discussions, and acknowledge support from the Harvard Society of Fellows.

-
- [1] D. J. Thouless *et al.*, Phys. Rev. Lett. **49**, 405 (1982).
 - [2] C. L. Kane and E. J. Mele, Phys. Rev. Lett. **95**, 226801 (2005).
 - [3] L. Fu, C. L. Kane and E. J. Mele, Phys. Rev. Lett. **98**, 106803 (2007).
 - [4] J.E. Moore and L. Balents, Phys. Rev. B **75**, 121306(R) (2007).
 - [5] R. Roy, Phys. Rev. B. **79**, 195322 (2009)
 - [6] L. Fu and C.L. Kane, Phys. Rev. B **76**, 045302 (2007).
 - [7] M. Z. Hasan and C. L. Kane, arXiv:1002.3895 (to appear in Rev. Mod. Phys.)
 - [8] J. E. Moore, Nature **464**, 194 (2010).
 - [9] X. L. Qi and S. C. Zhang, arXiv:1008.2026
 - [10] A. Schynder, S. Ryu, A. Furusaki and A. Ludwig, Phys. Rev. B **78**, 195125 (2008).
 - [11] A. Kitaev, arXiv:0901.2686
 - [12] R. K. Mong, A. M. Essin and J. E. Moore, Phys. Rev. B **81**, 245209 (2010).
 - [13] Y. D. Chong, X.-G. Wen, and M. Soljacic, Phys. Rev. B, **77**, 235125 (2008).
 - [14] K. Sun *et al*, Phys. Rev. Lett. **103**, 046811 (2009)
 - [15] To be precise, the tight-binding Hamiltonian should be regarded as operating on Wannier functions. For the bands we consider, their Wannier functions have the same symmetry as (p_x, p_y) orbitals.
 - [16] By including p_z orbitals, non-degenerate surface states can also be present. Strong hybridization with these additional states can eventually destroy the original gapless surface states.

- [17] C. L. Kane, Nat. Phys. **4**, 348 (2008).
- [18] X. G. Wen, *Quantum Field Theory of Many-Body Systems*, Oxford Press, 2004.
- [19] Z. Gu and X. G. Wen, Phys. Rev. B **80**, 155131 (2009);
F. Pollman *et al*, Phys. Rev. B **81**, 064439 (2010).
- [20] H. Yao and S. A. Kivelson, arXiv:1008.1065